Breeding and Solitary Wave Behavior of Dunes

O. Durán [1], V. Schwämmle [1,2] and H. Herrmann [1,3]
[1] *ICP, University of Stuttgart, 70569 Stuttgart, Germany*
[2] *Instituto de Física, Universidade Federal Fluminense, Av. Litorânea s/n, Boa Viagem; Niterói 24210-340, RJ, Brazil. and*
[3] *Departamento de Física, Universidade Federal do Ceará, 60455-970 Fortaleza, Brazil*

(Dated: February 2, 2008)

Beautiful dune patterns can be found in deserts and along coasts due to the instability of a plain sheet of sand under the action of the wind. Barchan dunes are highly mobile aeolian dunes found in areas of low sand availability and unidirectional wind fields. Up to now modelization mainly focussed on single dunes or dune patterns without regarding the mechanisms of dune interactions. We study the case when a small dune bumps into a bigger one. Recently Schwammle & Herrmann (*Solitary wave behavior of sand dunes.* Nature **426**, 610 (2003)) and Katsuki *et al.*(*Collision dynamics of two Barchans dunes simulated by a simple model.* cond-mat 0403312 (2004)) have shown that under certain circumstances dunes can behave like solitary waves. This means that they can "cross" each other which has been questioned by many researchers before. In other cases we observe coalescence, i.e. both dune merge into one, breeding, i.e. the creation of three baby dunes at the center and horns of a Barchan, or budding, i.e. the small dune, after "crossing" the big one, is unstable and splits into two new dunes.

PACS numbers: 45.70.Qj,45.70.Vn,89.20.-a

I. INTRODUCTION

We observe many different dune patterns in nature, as for example longitudinal, transverse, star and Barchan dunes. In regions where the wind blows mainly from the same direction sand availability determines the dune pattern. At high sand disposal transverse dunes dominate in the fields. They seem to be translationally invariant so that the lateral sand flux can be neglected. When less sand is available, Barchan dunes appear (Fig. 1). These are highly mobile having the form of a crescent moon. Their velocity can reach up to several tenths of meters per year and is proportional to the reciprocal height, meaning that smaller dunes are faster than large ones. The surface of a Barchan can be divided into different sections: the windward side, the slip face after the brink and the horns from which sand can leave the dune. Barchan dunes of different sizes are not perfectly shape invariant and there exists a minimal height of 2-3 meters below which they are not stable. These observations result from field measurements that have been made over the last decades [1, 2, 3, 4, 5, 6, 7]. Still many questions on dune dynamics remain open. Due to the large time scales involved in dune formation, full evolution of a dune is difficult to assess through measurements. Attempts have been made to get more insight through numerical calculations. Recently, several numerical models have been proposed in order to explain dune morphology and formation [8, 9, 10, 11, 12, 13, 14, 15, 16, 17, 18, 19, 20, 21]. They have to deal with the calculation of the turbulent wind field, the saltation sand flux over the windward side and the avalanches going down the slip face. Up to now modelization mainly focussed on single dunes or dune patterns without regarding the mechanisms of dune interactions.

Recently, Besler found small Barchans at the downwind side of big ones and concluded that Barchan dunes could behave like solitons [22, 23]. This means that they would behave like solutions of non-linear equations, for example those describing waves in shallow water, which propagate through each other without changing their shape [24]. As an example see Fig. 1. In (a) and (b) a small Barchan is apparently ejected from the main dune, whereas, in (c) small dunes emerge from the horns. Note the similarity with the snapshots of a collision simulation depicted in (b). Similar occurrences can be found in experiments with sub-aqueous Barchans [27]. Nevertheless, most researchers believe that if a small Barchan hits a bigger one, it will be completely absorbed. This is motivated by the fact that a sand formation cannot cross the slip face of a dune without being destroyed. Therefore the description of Barchan dunes as solitons has found very little support up to now, until Schwämmle et al. found that dunes can behave as solitary waves under certain

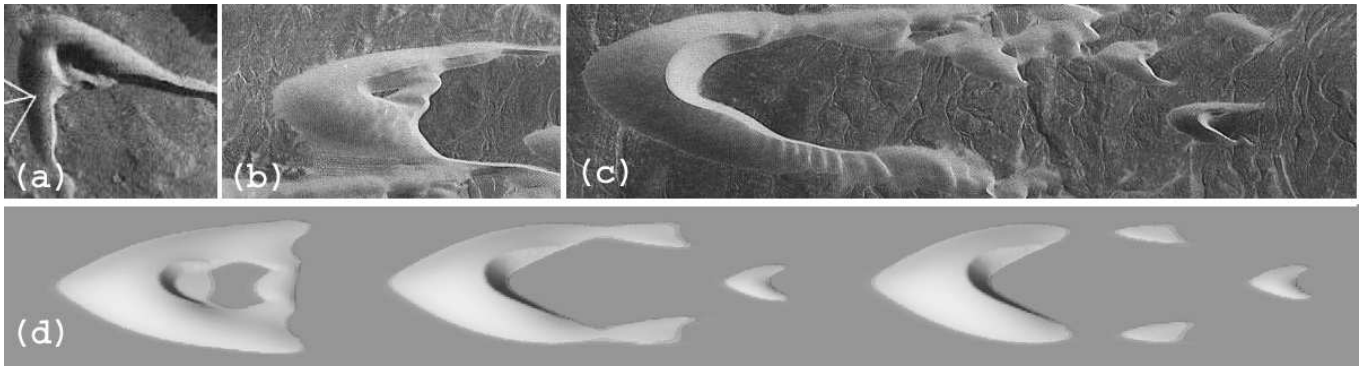

FIG. 1: Examples of the breeding process in two Barchan fields, Namibia (a) and Peru (b), (c), and in numerical simulations (c).

conditions [25]. They show that, due to mass exchange, a big Barchan colliding with a smaller one placed behind, may decrease its height until it becomes smaller, and therefore, faster, than the previous one, and leaves. Meanwhile the initially smaller dune increases its height becoming bigger and slower, in such a way that it looks as if the smaller dune crosses the big one. This situation was referred as solitary wave behavior. Katsuki et al. [26] also have obtained solitary wave behavior for coaxial and offset collisions of two sub-aqueous Barchans.

In the following we use a minimal model for dunes to develop the morphological phase diagram for the coaxial collision between two Barchans. We also characterize the transition between the different regimes using two order parameters and show a possible size selection mechanism in Barchan fields.

II. MODEL

Our model [16, 19, 21] consists of three coupled equations of motion calculating the shear stress of the wind field, the sand flux , the avalanche flux and the resulting change of the topography using mass conservation. The shear stress of the wind is obtained from the perturbation of the air flow over a smooth hill using the well known logarithmic velocity profile of the atmospheric boundary layer [31]. The shear velocity describes the strength of the wind. At the windward side of a Barchan dune the sand grains are transported by the so called saltation mechanism [1]. Below the big vortex of the wind field behind the brink the air cannot maintain sand transport. So the grains are deposited behind the brink in the lee zone of the Barchan until the surface reaches the angle of repose on which the sand flows down the slip face through avalanches.

The simulations are carried out with a completely unidirectional and constant wind source. In every iteration the horizontal shear stress $\boldsymbol{\tau}$ of the wind, the saltation flux $\mathbf{q}$ and the flux due to avalanches are calculated. The time scale of these processes is much shorter than the time scale of changes in the dune surface so that they are treated to be instantaneous. We perform all simulations using open boundary conditions with a constant influx. In the following the different steps at every iteration are explained.

a. The air shear stress τ on the ground: The shear stress is computed according to an analytical work describing the perturbation of the ground shear stress by a low hill or dune [28]. This perturbation is given by:

$$\begin{aligned}\tilde{\hat{\tau}}_x &= \frac{\tilde{h}_s\, k_x^2}{|\boldsymbol{k}|}\frac{2}{U^2(l)}\left\{-1+\left(2\ln\frac{l}{z_0}+\frac{|k|^2}{k_x^2}\right)\sigma\,\frac{K_1(2\sigma)}{K_0(2\sigma)}\right\},\\ \tilde{\hat{\tau}}_y &= \frac{\tilde{h}_s\, k_x\, k_y}{|\boldsymbol{k}|}\frac{2}{U^2(l)}\,2\sqrt{2}\,\sigma K_1\big(2\sqrt{2}\,\sigma\big)\,, \qquad (1)\end{aligned}$$

where $\sigma=\sqrt{i\,L\,k_x\,z_0/l}$.

Here, K_0 and K_1 are modified Bessel functions. k_x and k_y are the components of the wave vector $\boldsymbol{k}$, the coordinates in Fourier space. $\tilde{\hat{\tau}}_x$ and $\tilde{\hat{\tau}}_y$ are the Fourier-transformed components of the shear stress perturbation in wind direction and in transverse direction. $\tilde{h}_s$ is the Fourier transform of the height profile, U is the vertical velocity profile which is suitably nondimensionalised, l the depth of the inner layer of the flow, and z_0 the roughness length which takes into account saltation. L is a typical length scale of the hill or dune and is given by a quarter of the mean wavelength of the Fourier representation of the height profile. In order to take into

account the shear stress strong reduction in the lee side of the hill, where the linear models overestimate it [29], we multiplied the imaginary part of $\tilde{\hat{\tau}}_x$ by the fenomenological constant 1.5.

It has to be taken into account that the flow separates at the brink of the slip face of a dune. This is done by assuming an idealized "separation bubble", a region inside which there is no flow and outside of which the air flows as over a shape of the combined dune and bubble. Each slice in wind direction of the bubble is modelled by a third-order polynomial so that in the case of a barchan the region between the horns is inside the bubble. The height profile h_s in (1) is the profile of the dune including the separation bubble.

b. The saltation flux q: From the shear stress, the modification of the air flow due to the presence of saltating grains is accounted for. This results in an effective wind velocity driving the grains.

$$v_{\text{eff}} = \frac{u_{*t}}{\kappa}\left(\ln\frac{z_1}{z_0} + 2\left(\sqrt{1+\frac{z_1}{z_m}\left(\frac{u_*^2}{u_{*t}^2}-1\right)}-1\right)\right), \tag{2}$$

where $u_* = \sqrt{\tau/\rho_{\text{air}}}$

The shear stress $\boldsymbol{\tau}$ results from (1) through $\boldsymbol{\tau} = \boldsymbol{\tau}_0 + |\boldsymbol{\tau}_0|\,\hat{\boldsymbol{\tau}}$, where $\boldsymbol{\tau}_0$ is the shear stress over a flat plane. z_0 is the roughness length of the sand excluding the effect of saltation, and $\kappa \approx 0.4$ is von Kármán's constant. z_m, the mean saltation height, and z_1 are parameters of the model.

The next step is the computation of the typical velocity of the saltating grains. It is determined by the balance between the drag force acting on the grains, the loss of momentum when they splash on the ground, and the downhill force. It is computed by solving the following quadratic vector equation numerically:

$$\frac{3}{4}\,C_d\frac{\rho_{\text{air}}}{\rho_{\text{quartz}}}d^{-1}\,(\mathbf{v}_{\text{eff}}-\mathbf{u})|\mathbf{v}_{\text{eff}}-\mathbf{u}| - \frac{g}{2\alpha}\frac{\mathbf{u}}{|\mathbf{u}|} - g\,\boldsymbol{\nabla}\,h = 0, \tag{3}$$

where $\mathbf{v}_{\text{eff}} = v_{\text{eff}}\frac{\mathbf{u}_*}{|\mathbf{u}_*|}$. C_d is the drag coefficient of a grain. d_{grain} and ρ_{grain} are the diameter and the density of the grains. α is a model parameter.

The sand flux due to saltation is then obtained by numerically solving the transport equation:

$$\operatorname{div}\mathbf{q} = \frac{1}{l_s}q\left(1-\frac{q}{q_s}\right)\begin{cases}\Theta(h) & q<q_s\\ 1 & q\geq q_s\end{cases}, \tag{4}$$

with

$$q_s = \frac{2\alpha}{g}\,|\mathbf{u}|\,(|\boldsymbol{\tau}|-\tau_t) \qquad l_s = \frac{2\alpha|\mathbf{u}|^2}{\gamma g}\,\frac{\tau_t}{(|\boldsymbol{\tau}|-\tau_t)}. \tag{5}$$

Here g is the gravity acceleration, and α, β and γ are model parameters taken from [32].

c. The time evolution of the surface: When the sand flux has been calculated, the height profile is updated according to the mass conservation:

$$\frac{\partial h}{\partial t} = -\frac{1}{\rho_{\text{sand}}}\operatorname{div}\mathbf{q}. \tag{6}$$

d. Avalanches: In the last step, avalanches are simulated where necessary. If the slope of the sand surface exceeds the static angle of repose, sand is redistributed according to the sand flux:

$$\mathbf{q}_{\text{aval}} = E\,(\tanh|\nabla h| - \tanh(\tan\theta_{\text{dyn}})\,\frac{\nabla h}{|\nabla h|} \tag{7}$$

The surface is repeatedly changed according to (6) using this flux, until the maximum slope is below the dynamic angle of repose, θ_{dyn}. The hyperbolic tangent function serve only to improve convergence.

All these steps are repeated iteratively to simulate the evolution of the shape.

III. RESULTS

We performed calculations by numerically solving the set of equations initially placing a big Barchan (volume V_H) downwind of a smaller one (volume V_h). The strength of the wind blowing into the system is fixed to a shear velocity of 0.5 m/s. The influx is 0.001 kg/ms, equal to the big Barchan equilibrium outflux. In order to take into account the lack of scale invariance of Barchans, we repeat the simulations for two different sizes of the big Barchan, with initial volumes V_H: 6 and 70 $\times 10^3 m^3$. The same general picture was observed. The smaller Barchan at some point bumps into the larger one. This leads to a hybrid state where the two dunes melt into a complex pattern. Four different situations can be observed: coalescence (Fig. 2a), breeding (Fig. 2b and 2c), budding (Fig. 2d) and solitary wave behavior (Fig. 2e) depending only on the relative sizes of the two dunes. Thus, we chose as control parameter the relative volume between the two dunes V_h/V_H.

The evolution of the hybrid state can be understood as the result of a competition between two processes. The first one is the overlapping of both dunes at the beginning of the collision that eventually can lead to coalescence (Fig. 3, upper part). The second one is the effective mass exchange between the dunes due to the changes induced to the wind shear stress due to the approaching of both

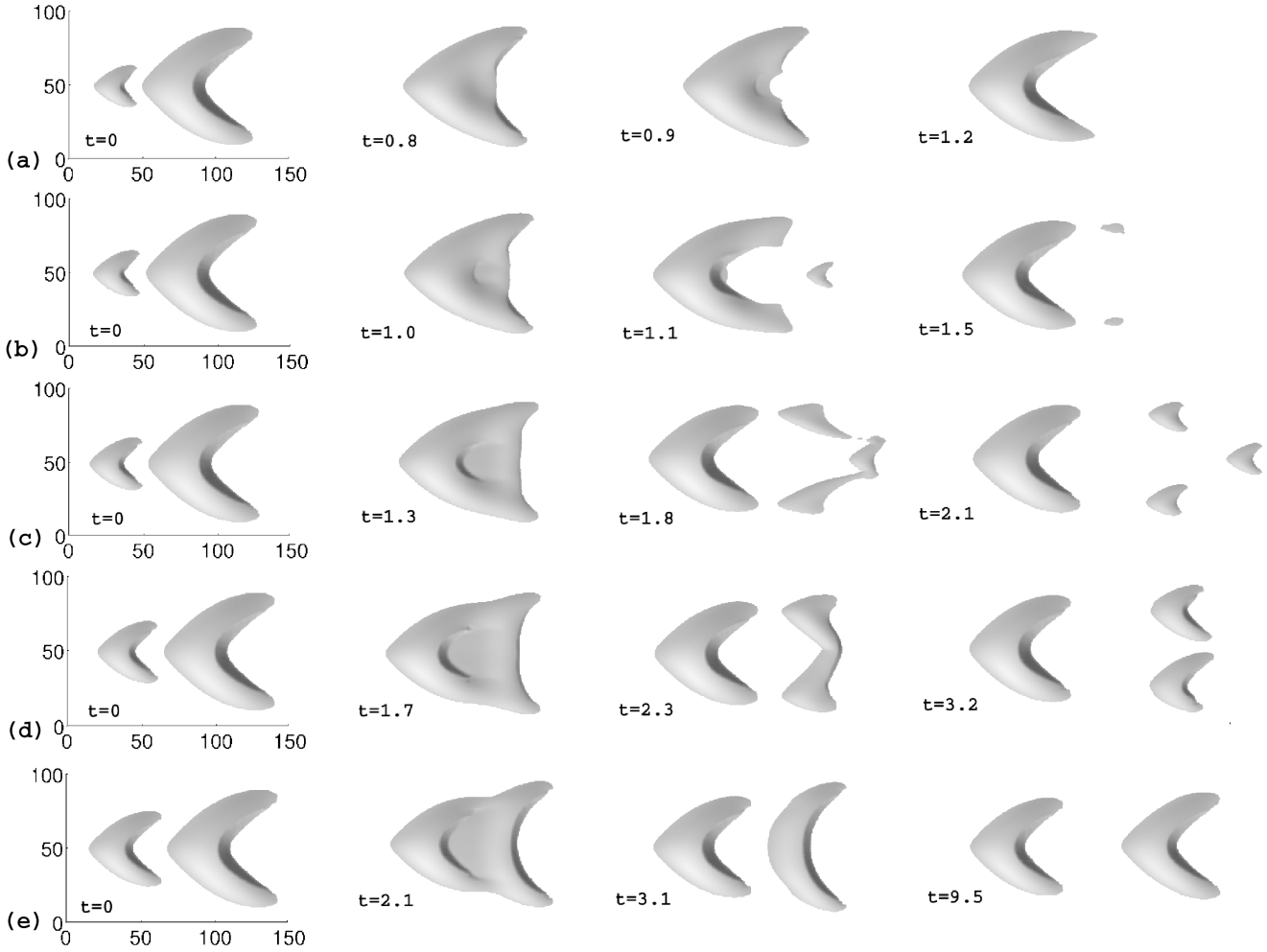

FIG. 2: Different situations during the collision of two Barchans for $(V_h/V_H)_i = 0.06$ (a), 0.08 (b), 0.12 (c), 0.17 (d) and 0.3 (e) using open boundary condition. Coalescence (a), breeding (b) and (c), budding (d) and solitary wave behaviour (e) take place. The time (t) is in month. The initial volume and height of the big Barchan is $6 \times 10^3 m^3$ and $5\,m$ height, whereas the heights of the smaller Barchan are $1.8\,m$ (a), $1.9\,m$ (b), $2.2\,m$ (c), $2.6\,m$ (d) and $3.1\,m$ (e).

dunes. In the hybrid state the wind shear stress over the windward side of the bigger dune is reduced and thus, crest erosion is enhanced. Besides, the wind shear stress over the lee side of the dune smaller is also reduced but enhancing crest deposition. Thus, the dune smaller may gain enough sand to become bigger than the one in front and therefore also becomes slower. In this way, the before bigger dune can become the smaller one and its velocity sufficiently large to leave the hybrid state. In this case the dunes separate again (Fig. 3, bottom).

The collision process is crucially affected by the separation bubble, i.e. the region after the brink and between the horns at which flow separation occurs (see item *a.* in the Model section). After the separation at the brink, the flow streamlines reattach smoothly near the line segment whose end points are the horns. There, sand transport continues again. However, inside the separation bubble the flow is strongly reduced and, for simplicity, we set the flux to zero. Hence, the upwind dune will absorb that part of the downwind dune inside its separation bubble (Fig. 2c, 2d and 2e).

For small relative volume ($V_h/V_H < 0.07$) both dunes coalesce to a single one. In this case the relative velocity is high and hence the overlapping is faster than their mass exchange. Small dunes have a short slip face which disappears while climbing up the bigger one. This reduces the mass exchange and leads to a complete absorption of very small Barchans (Fig. 2a). For larger V_h/V_H the

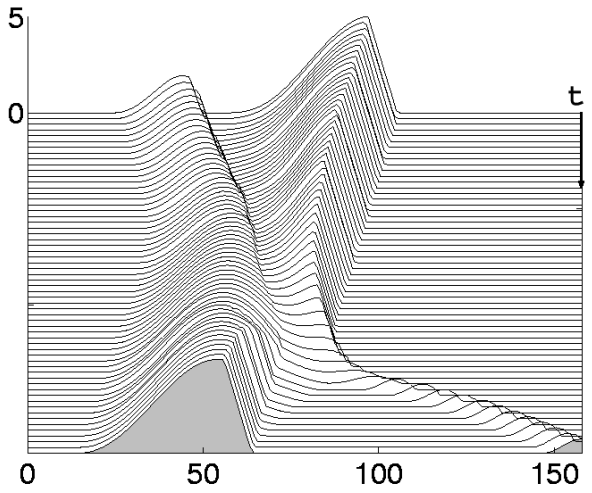

FIG. 3: Time evolution of the central slice of the 'breeding' collision represented in the figure 2b. Note initially the small dune climbing on the biger one, and finally their mass exchange that leads to their separation.

slip face survives for longer time, mass exchange becomes relevant, and a small barchan is ejected from the central part of the dune (Fig. 3). The perturbation of the big dune shape, due to the overlapping of the small dune behind, also propagates over the horns since there is no slip face. At the end of each horn a small dune is ejected. This phenomenon of triple ejection we call 'breeding'. Fig. 2b shows the snapshots. Note the qualitative similarity with the Barchan field shown in Figure 1.

As the relative volume increases ($V_h/V_H > 0.14$), a smaller relative velocity favours the mass exchange and reduces the overlapping process, leading to the complete separation of both dunes. Nevertheless, the leaving dune lacks the central part of its windward side and cannot reach the stable Barchan shape. Therefore, it splits into two new dunes, a phenomenon we call 'budding' (Fig. 2d). A similar phenomena was reported in experiments with sub-aqueous Barchans [27].

Between the 'breeding' and 'budding', a transition occurs at which the 'breeding' three ejected dunes are connected forming a single dune that, afterwards, splits into three again (Fig. 2c). For a higher relative volume the central ejected dune decrease its size until disappear at 'budding'. We consider this transition also as 'breeding'.

When V_h/V_H is greater than 0.25, the instability of the dune in front disappears and both dunes develop to Barchans. Then, we observe solitary wave behavior as shown in Figure 2e. In that case the dunes move with similar velocity and the mass exchange is the main process of the evolution of the hybrid state. The overlapping of both dunes is very small now and the emerging dune looses merely a small fraction of its tail. Effectively it looks as if the smaller dune just crosses the bigger one while in reality due to mass exchange the two heaps barely touches each other.

The morphological phase diagram crucially influences the evolution of the number of dunes in a Barchan field. In the coalescence region ($V_h/V_H < 0.07$) the number of dunes decreases by one, whereas three dunes in the breeding ($0.07 < V_h/V_H < 0.14$) and two dunes in the budding region ($0.14 < V_h/V_H < 0.25$) appear, and the number of dunes increases by two and one respectively. Finally, in the solitary waves region ($0.24 < V_h/V_H$) a small dune seems to cross the bigger one and the number of them remains constant.

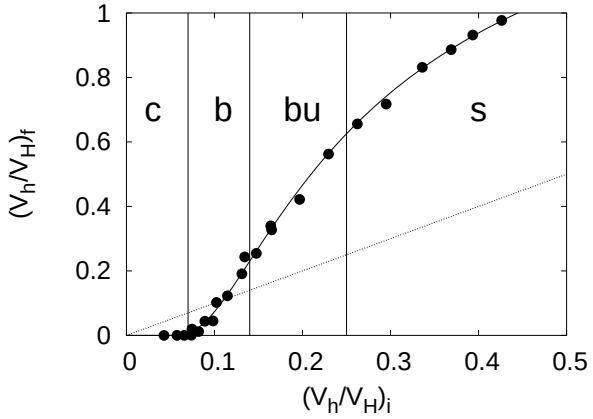

FIG. 4: Relation between the relative volume of the dunes before ($(V_h/V_H)_i$) and after the collision ($(V_h/V_H)_f$). The regions in the morphological phase diagram are showed: coalescence (c), breeding (b), budding (bu) and solitary waves (s). For coalescence only one dune emerges and thus, the relative volume is zero, whereas for breeding, budding and solitary waves the relative volume seems to follow a exp(-1/x) law (full line).

In order to analyze the transition type between any two regimes, we introduce two order parameters, the relative volume after the collision ($(V_h/V_H)_f$) for the 'coalescence-breeding' transition, and the inverse of time during which the emerging dune does not split, for the 'budding-solitary waves' transition. Note that the former parameter is zero for coalescence, where no dunes emerge, and the later one is zero for solitary wave behavior, where the leaving dune evolves into a Barchan shape without splitting.

Figure 3 shows the relative volume after the collision

as a function of the initial one, approximately related by the formula:

$$\left(\frac{V_h}{V_H}\right)_f \propto \exp\left(\frac{-0.22}{\left(\frac{V_h}{V_H}\right)_i - r_c}\right) \quad (8)$$

where $r_c = 0.03$. This suggests an essential singularity in the 'coalescence-breeding' transition. It implies that the volume of the leaving dune in the budding regime does not have a minimum value, thus, after a Barchan it is possible to find small dunes of any height.

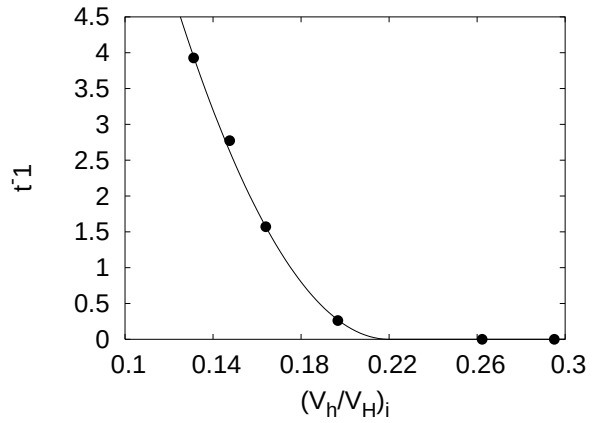

FIG. 5: Inverse of the time during which the emerging dune does not split, as a function of the initial relative volume. By definition, this time is infinitely long for the solitary wave behavior. Note the continuity at the transition from budding to solitary waves, suggesting a second order transition.

On the other hand, Figure 5 shows the inverse of the time during which the emerging dune does not split. The continuity of the curve at the 'budding-solitary wave' transition suggest a second order transition. Near the transition point the leaving dune splits in a infinite time. Thus, we cannot define in a Barchan field a characteristic length for the budding process.

It is interesting to note that the relative volume increases after a solitary wave collision (Fig. 4). The collision process redistributes the initial mass making both dunes more similar, giving rise to a size selection mechanism in Barchan fields [18]. However, due to the permanent exchange of sand between the dunes, their sizes are not constant after the collision and change with their influx and thus with the selected boundary condition. Furthermore, the open problem of its stability [18] introduces another uncertainty about their final sizes.

IV. CONCLUSIONS

In this work we develop a morphological phase diagram showing that during the collision of two Barchans four situations can be observed: coalescence, breeding, budding and solitary waves (Fig. 2: a, b, c, d and e). At large scales the collision process depicted here could lead to a selection of a characteristic size of dunes in a Barchan field. However, we only considered perfectly aligned dunes.

Calculations of very large dune fields are still difficult because of high computational costs. One way out would be to consider a simplified model containing the main features of dune movement and interaction. For that purpose one could use the collision rules obtained in this work on a larger scale [33].

Acknowledgments

We thank E. Parteli and A. O. Sousa for stimulating discussions and Max Plank Price and DAAD for financial support.

[1] Bagnold, R. A. *The Physics of Blown Sand and Desert Dunes.* Methuen, London, (1941).

[2] Finkel, H. J. *The Barchans of southern Peru.* Journal of Geology **67**, 614-647 (1959).

[3] Coursin, A. *Observations et expériences faites en avril et mai 1956 sur les barkhans du Souehel el Abiodh (région est de Port-Étienne).* Bulletin de l' I. F. A. N. 22A, no. 3, 989-1022 (1964).

[4] Hesp, P. A. & Hastings, K. *Width, height and slope relationships and aerodynamic maintenance of barchans.* Geomorphology **22**, 193-204 (1998).

[5] Jimenez, J. A., Maia, L. P., Serra, J. & Morais, J. *Aeolian dune migration along the Ceará coast, north-eastern Brazil.* Sedimentology **46**, 689-701 (1999).

[6] Sauermann, G., Rognon, P., Poliakov, A. & Herrmann, H. J. *The shape of the barchan dunes of southern Morocco.* Geomorphology **36**, 47-62 (2000).

[7] Sauermann, G. et al. *Wind velocity and sand transport on a barchan dune.* Geomorphology, (2003).

[8] Wippermann, F. K. & Gross, G. *The wind-induced shaping and migration of an isolated dune: A numerical experiment.* Boundary Layer Meteorology **36**, 319-334

(1986).

[9] Zeman, O. & Jensen, N. O. *Progress report on modeling permanent form sand dunes.* Risø National Laboratory M-2738 (1988).

[10] Fisher, P. F. & Galdies, P. *A computer model for barchan-dune movement.* Computer and Geosciences 14-2, 229-253 (1988).

[11] Stam, J. M. T. *On the modelling of two-dimensional aeolian dunes.* Sedimentology **44**, 127-141 (1997).

[12] Nishimori, H., Yamasaki, M. & Andersen, K. H. *A simple model for the various pattern dynamics of dunes.* Int. J. of Modern Physics B **12**, 257-272 (1999).

[13] van Boxel, J. H., Arens, S. M. & van Dijk, P. M. *Aeolian processes across transverse dunes i: Modelling the air flow.* Earth Surf. Process. Landforms **24**, 255-270 (1999).

[14] van Dijk, P. M., Arens, S. M. & van Boxel, J. H. *Aeolian processes across transverse dunes ii: Modelling the sediment transport and profile development.* Earth Surf. Process. Landforms **24**, 319-333 (1999).

[15] Momiji, H. & Warren, A. *Relations of sand trapping effciency and migration speed of transverse dunes to wind velocity.* Earth Surface Processes and Landforms **25**, 1069-1084 (2000).

[16] Kroy, K., Sauermann, G. & Herrmann, H. J. *Minimal model for sand dunes.* Phys. Rev. L. **88**, 54301 (2002).

[17] Andreotti, B., Claudin, P. & Douady, S. *Selection of dune shapes and velocities* Eur. Phys. J. B **28**, 315-339 (2002).

[18] Hersen, P. et al. *Corridors of barchan dunes: stability and size selection.* Phys. Rev. E. **69**, 011304 (2004).

[19] Schwämmle, V. & Herrmann, H. *Modelling transverse dunes.* cond-mat 0301589, (2003).

[20] Schwämmle, V. & Herrmann, H. *A model of barchan dunes including lateral shear stress.* cond-mat 0304695, (2003).

[21] Sauermann, G., Kroy, K. & Herrmann, H. J. *A continuum saltation model for sand dunes.* Phys. Rev. E **64**, 31305 (2001).

[22] Besler, H. *Eine Wanderdüne als Soliton?* Physikalische Blätter. **10**,983 (1997).

[23] Besler, H. *Complex barchans in the Libyan desert: dune traps or overtaking solitons?* Zeitschrift für Geomorphologie N.F. **126**, 59-74 (2002).

[24] Lamb, G. L. *Elements of Soliton Theory.* Wiley, (1980).

[25] Schwämmle, V. & Herrmann, H. *Solitary wave behaviour of sand dunes.* Nature **426**, 610 (2003).

[26] Katsuki, A., Nishimori, H., Endo, N. & Taniguchi, K. *Collision dynamics of two barchans dunes simulated by a simple model.* cond-mat 0403312 (2004).

[27] Endo, N. & Taniguchi, K. *Obsevation of the whole process of interaction between barchans by flume experiments.* Geophysical Research Letters **34**, L12503 (2004).

[28] Weng, W. S. et al. *Air flow and sand transport over sand-dunes.* Acta Mechanica (Suppl.)**2**, 1-22 (1991).

[29] Hewer, F.E. *Non-linear numerical model predictions of flow over an isolated hill of moderate slope.* Boundary Layer Meteorology **87**, 381-408 (1998).

[30] Bouchaud, J. P., Cates, M. E., Ravi Prakash, J. & Edwards, S. F. *Hysteresis and metastability in a continuum sandpile model.* J. Phys. France I **4**, 1383 (1994).

[31] Prandtl, L. *The mechanics of viscous fluids. in Aerodynamic Theory*, (Durand, W. F., ed) volume Vol. III, 34-208. Springer, Berlin (1935).

[32] Sauermann, G. *Modeling of wind blown sand and desert dunes.* PhD thesis, University of Stuttgart (2001).

[33] Lima, A. R., Sauermann, G., Kroy, K.& Herrmann, H. J. *A model for dune fields.* Physica A **310**, 487-500 (2002).